THREE-DIMENSIONAL (3D) MICROSTRUCTURE VISUALIZATION AND FINITE ELEMENT MODELING OF THE MECHANICAL BEHAVIOR OF HETEROGENEOUS MATERIALS

N. Chawla and V.V. Ganesh

Department of Chemical and Material Engineering
Ira A. Fulton School of Engineering
Arizona State University
Tempe, AZ 85287-6006 USA

ABSTRACT

A serial sectioning process was used to develop a three-dimensional (3D) representation of the microstructure of a SiC particle reinforced Al composite, for visualization and finite-element modeling (FEM). The Young's modulus and stress-strain behavior of the composite predicted by the 3D model of microstructure correlated very well with experimental results.

1 INTRODUCTION

Silicon carbide particle reinforced aluminum composites exhibit high strength and stiffness by combining strong, ceramic reinforcement particles in a soft aluminum matrix [1]. SiC particle size, morphology, and orientation with respect to the loading axis play a significant role in determining the stiffness, strength, and fatigue resistance of the composite [1-4]. Traditional methods of visualizing the microstructure of composites as well as other materials involve simplifying the three-dimensional (3D) structure to a two-dimensional (2D) representation by optical or scanning electron microscopy (SEM). While 2D representation of microstructures is common and gives some idea of the microstructure morphology, it is not fully representative of the 3D structure of the material. Therefore, to visualize and fully understand a material's microstructure, a technique that can capture the 3D nature of the microstructure is required. Serial sectioning is a technique that allows the quantification of 3D microstructures using classical metallography techniques coupled with computer-aided reconstruction [5]. Recently, computer-aided serial sectioning techniques have been used to study several material systems, including Al-Si [6], proeutectoid iron alloy [7], and SiC/Al composites [8].

While visualization of the 3D microstructure of the material is important, prediction of the behavior and properties of the material is equally important. Thus, a microstructure-based modeling approach is required to link the microstructure with the behavior of the material. Numerical modeling of the behavior of Al/ SiC_p composites has typically been conducted by assuming a single SiC particle of simple geometry in a unit cell model [1, 3, 9]. Unit cell

models approximate the highly variable and angular structure of SiC particles using simplified particle geometries such as spheres, ellipsoids, or cubes. This simplification aids in computation but fails to capture the complex morphology, size, and spatial distribution of SiC particles in the Al matrix. It follows that an accurate simulation of the material behavior can only be obtained by incorporating actual 3D microstructure morphologies as a basis for the model.

Here we have used a microstructure-based modeling approach by combining serial sectioning and computer-aided reconstruction with 3D finite element modeling (FEM). Serial sectioning was used to reveal the 3D microstructure of SiC particle reinforced aluminum matrix composites. The reconstructed 3D microstructure obtained was then used as a basis for 3D FEM modeling of uniaxial tensile behavior. The process allowed 3D visualization of SiC particles as well as intrinsic and accurate microstructure-based modeling of the behavior of SiC/Al composites. It will be shown that the 3D microstructure of the composite is more accurate in predicting and visualizing the mechanical behavior of the composite than the simple SiC particle geometry employed in conventional unit cell models.

2 EXPERIMENTAL PROCEDURE

In this work a 20 vol.% SiC reinforced 2080 aluminum composite processed by hot-pressing and extrusion (Alcoa Corp.) was examined. The SiC particles in the composite had an average particle size of about 8 μm (after extrusion). The SiC/Al composite samples were cut so that the extrusion axis was parallel to the cutting plane (longitudinal axis). A serial sectioning method was employed to acquire 2D images of the microstructure as a basis for reconstructing 3D microstructure of the composite for modeling using FEM. The basic steps of the serial sectioning process and modeling were as follows:

1. Sample preparation
2. Fiducial marking by indentation
3. Polishing
4. Imaging and image segmentation
5. Serial section stacking and visualization
6. Finite element modeling

The SiC/Al samples were cut and mounted for polishing. A representative region of the microstructure was selected, denoted here as the region of interest. Selection of the region of interest was important because it defined the volume of microstructure to be analyzed. A “representative” volume is a very subjective assessment that is based on the microstructural feature size and computational capability [6]. In the composite studied here, it was desirable to obtain several SiC particles included in the analyzed volume. Thus, since the SiC particles were about 8 μm in diameter, it was determined that a 100 μm x 100 μm x 10 μm volume would yield a representaive group of particles for reconstruction and modeling.

Fiducial marks were made by Vickers indentation. These marks were used to measure the material thickness loss during polishing/grinding. Since the geometry of the indenter is known, the amount of material thickness removed can be calculated from the geometry of the indenter. Measurements of changes in the fiducial mark depth were used to determine the thickness between sections from material loss per polishing cycle. The average cumulative thickness loss rate, taken as the average of indentations at the four corners of the region of interest, was about 1 μm per cycle. Since the size of the microstructural features dictates the thickness between sections, with SiC particles about 8 μm in diameter, this would give about 5-6 sections per particle in the analyzed volume. Cyclic polishing and imaging of the sample surface were then conducted to generate a series of microstructural sections. These details are given elsewhere [10,11].

After each polishing cycle, optical micrographs of the microstructure were segmented into black-and-white images using standard image analysis technique. The sample was secured using a mounting fixture to minimize translational and rotational artifacts between sections. In order to simplify the microstructure for FEM, the 3D particles were simplified using a vectoral format software (Surf Driver). These simplifications did not significantly change the original morphology of the SiC particles, as described elsewhere [10,11]. The 3D model was exported into a computer-aided drawing (CAD) software and then into the finite element analysis program (ABAQUS/CAE, version 6.3-1, HKS, Inc., Pawtucket, RI). Ten noded, modified quadratic tetrahedral elements were used in the elastic-plastic analysis of the composite, particularly to conform to the irregular shape of the particles. Mesh refinement was conducted by gradually increasing the number of elements and quantifying the overall stress-strain curve. A typical number of elements in the 3D model was about 76,000 elements. All FEM analysis was conducted on a PC computer with dual 1.7 GHz processor, and 2 GB of RAM. Two microstructural models were built from two different regions of the material, to quantify the extent of microstructural variability on the modeled macroscopic stress-strain behavior.

3 RESULTS AND DISCUSSION

Figure 1(a) shows a multi-particle reconstruction, where several of the particles are clearly aligned along the extrusion axis. The 3D model of the microstructure with 14 particles was used as a basis for FEM analysis, Fig. 1(b). This model was compared with conventional 3D unit cell models where the SiC particle was perfectly spherical and perfectly rectangular, Fig. 2. The sphere had an aspect ratio of one, while the rectangular particle had an aspect ratio of about 2 (close to the average aspect ratio of the SiC particles). The SiC particles were modeled as linear elastic (Young's modulus, $E = 410$ GPa, Poisson's ratio, $\nu = 0.19$) while the experimentally-determined stress-strain curve for the unreinforced Al alloy (up to the ultimate tensile strength), was used as the input for the matrix. The Young's modulus and Poisson's ratio of the Al alloy, were 74 GPa and 0.33, respectively. A 2%

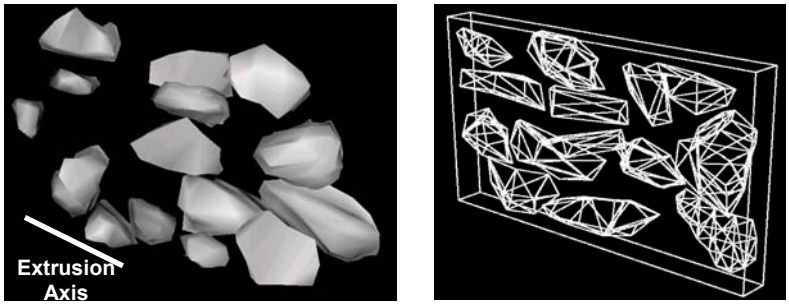

Figure 1. 3D reconstruction of the complex geometry SiC particles, showing clear alignment of particles along the extrusion axis.

uniaxial strain was applied to all models by fixing the displacement of the x-z plane in x, y, and z directions, and applying a uniaxial displacement on the parallel x-z plane in the x-direction. In the microstructure-based model, this corresponded to loading along the extrusion axis. The rotation of the model was also constrained along all three axes. Plasticity from thermal mismatch, between particle and matrix, during cooling of the composite from the processing temperature was also modeled by using a ΔT of 468 K ($493^{o}C - 25^{o}C$). The coefficients of thermal expansion of SiC and Al were taken as $4.3x10^{-6}$ and $22x10^{-6}$, respectively.

The macroscopic stress-strain behavior of all models is shown in Fig. 3. The highest and lowest simulated moduli and strength were obtained by the unit cell prismatic rectangle and sphere, respectively. This can be attributed to the highest degree of load transfer for the prismatic rectangular particle than the spherical particles [1]. The 3D microstructure models, from two different regions of the material, exhibited a higher degree of strengthening, since the actual microstructure incorporated the inherent aspect ratio and alignment of the SiC particles along the loading direction. A comparison of all predicted moduli with experimental tensile data on the same composite, from Ganesh and Chawla [2], is shown in Table 1. The two 3D microstructure models correlate very well with the experimentally determined Young's modulus value of 108 GPa. A comparison of the overall stress-strain curve (elastic and plastic parts) of the 3D microstructure simulation to the experiment is shown in Fig. 3. These simulations incorporated a cooling step in the

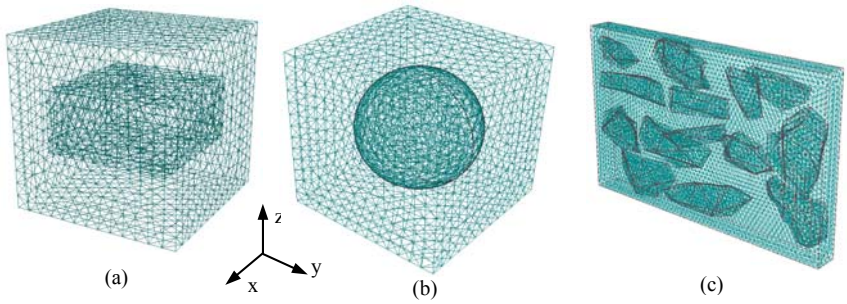

Figure 2. Models evaluated in finite element simulations: (a) prismatic unit cell, (b) spherical unit cell, and (c) microstructure.

model, from the solution treating temperature of 493°C to 25°C. The prismatic rectangle and microstructure-based models both predict the experimental behavior quite well. Nevertheless, the microstructure-based models more faithfully represent the experimental behavior. It should be noted that the microstructure-based model used here contains only a single "layer" of particles. Experimentally, this layer would be surrounded by a larger number of particles, which could potential add some constraint to the particles in the layer. The contribution that a larger number of modeled particles may have in influencing constraint in the model is unclear. Current work is exploring the effects of number of particles and size of volume modeled on the overall stress-strain response of the model [12]. Nevertheless, the very good agreement between the stress-strain behavior of the model presented here, with that of the experiment, lead us to believe that the contribution from constraint of adjacent particles appears to be small. Thus, the microstructure-based models appear to be a reasonable representation of the actual 3D microstructure.

Figure 4 shows the evolution of equivalent plastic strain showing the onset of plastic flow at sharp angular corners of the particles, followed by localization of strain between particles. The plastic deformation became concentrated at the poles of the particles along the loading axis, as predicted by Goodier [13]. It is also interesting

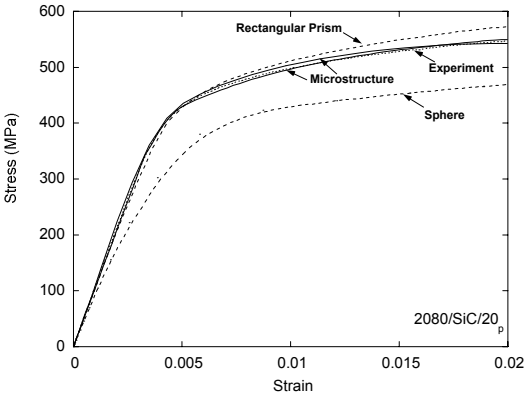

Figure 3. Comparison of stress-strain predictions from various FEM models after thermal cooling. The 3D microstructure models (from two random regions in the microstructure) is most accurate in predicting the experimentally observed behavior.

Table 1. Young's Modulus Predicted by Various Finite Element Models

3D Model or Experiment	Young's Modulus (GPa)
Unit Cell - Rectangle	113
Unit Cell - Sphere	100
Microstructure	107.4 ± 0.4
Experiment [2]	107.9 ± 0.7

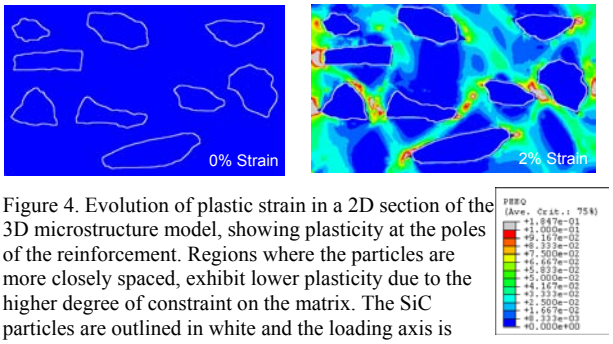

Figure 4. Evolution of plastic strain in a 2D section of the 3D microstructure model, showing plasticity at the poles of the reinforcement. Regions where the particles are more closely spaced, exhibit lower plasticity due to the higher degree of constraint on the matrix. The SiC particles are outlined in white and the loading axis is horizontal.

to note that within a region where the particles are more closely spaced, there is a lack of plasticity due to the large degree of constraint on the matrix in these regions.

4 CONCLUSIONS

The following conclusions can be made from this study to develop a serial sectioning methodology for visualization and FEM modeling of SiC particle reinforced Al composites:

- A serial sectioning process was used to reproduce and visualize the 3D microstructure of SiC particle reinforced aluminum composites. The 3D microstructure accurately represented the orientation, aspect ratio, and distribution of the particles.
- FEM simulation of the uniaxial loading behavior of SiC particle reinforced aluminum composite was conducted on 3D unit cell particles (spherical and rectangular prism) and the 3D microstructure obtained from serial sectioning. The 3D microstructure models, from two regions of the microstructure, was the most accurate in predicting the Young's modulus of the composite.
- With the incorporation of thermal mismatch-induced plasticity, at the particle/matrix interface, in the FEM model, the 3D microstructures also predicted the overall stress-strain behavior of composite extremely well.
- The serial sectioning method, reconstruction, and FEM technique is an improvement over 2D and 3D unit cell models, and can be used to effectively visualize and simulate material behavior.

References

1. N. Chawla and Y.L. Shen, *Adv. Eng. Mater.*, (2001) **3** 357-370.
2. V.V. Ganesh and N. Chawla, *Metall. Mater. Trans.*, (2004) **35A** 53-62.
3. N.J. Sorensen, S. Suresh, V. Tvergaard, and A. Needleman, *Mater. Sci. Eng.,* (1995) **A197** 1-10.
4. H.K. Jung, Y.M. Cheong, H.J. Ryu, and S.H. Hong, *Scripta Mater.,* (1999) **41** 1261-1267.
5. L. Wojnar, **Image Analysis: Applications in Materials Engineering**, CRC Press, Boca Raton, FL, 1999.
6. J. Alkemper and P.W. Voorhees, *Journal of Microscopy*, (2001) **201** 388-394.
7. M.V. Kral and G. Spanos, *Scripta Materialia*, (1997) **36** 875-882.
8. M. Li, S. Ghosh, T. N. Rouns, H. Weiland, O. Richmond, and W. Hunt, *Materials Characterization* (1998) **41** 81-95.
9. Y.-L. Shen, A. Needleman, and S. Suresh, *Metall. Mater. Trans.*, (1994) **25A** 839.
10. B. Wunsch, X. Deng, and N. Chawla, in *Computational Methods in Materials Characterisation*, (A.A. Mammoli and C.A. Brebbia, eds.), (2004), WIT Press, Boston, pp. 175-184.
11. N. Chawla, V.V. Ganesh, and B. Wunsch, *Scripta Mater.*, (2004) **51** 161-165.
12. V.V. Ganesh and N. Chawla, (2003) unpublished work.
13. J. Goodier, *J. Appl. Mech.*, (1933) **39** 55-57.